

Calibration of very close range digital cameras

Aleksandra Bujakiewicz, Michal Kowalczyk, Piotr Podlasiak, Dorota Zawieska

Institute of Photogrammetry and Cartography
Warsaw University of Technology
1 Plac Politechniki, 00-661 Warsaw, Poland

e-mail: abujak7@wp.pl; mmkowalczyk@wp.pl; ppodlasiak@wp.pl; dorotaz8@wp.pl

Received: 10 January 2006/Accepted: 6 April 2006

Abstract: The paper discusses the problems of the calibration process of very close range semi-metric digital cameras. Using such cameras for precise measurement of small objects, the photographs have to be taken at a very large scale, ranging from 1:20 to 1:50. To ensure the submillimetre accuracy of the photogrammetric measurement, the specific calibration tests and procedures for determination of the interior orientation parameters, including the coefficients for image systematic errors, must be applied. The results of two calibration approaches, based on 3D and 2D calibration tests, have been presented in the paper. The experiment is a part of the research project concerning the numerical modelling of small 3D fragments of the broken archaeological items for reconstruction of the context of the archaeological monument.

Keywords: Close range photogrammetry, semi-metric camera, calibration

1. Introduction

Reconstruction and modelling of the surfaces of small three dimensional objects are quite common within the applications of close range photogrammetry. Objects such as some details of archaeological or industrial structures are usually of the size of 10–40 cm with the differences in Z coordinate from a few to several centimetres. The surface reconstruction requires a huge number of points to be measured automatically with submillimetre accuracy. On the market there are many different commercial close range systems, such as RolleiMetric CDW (*Close-range Digital Workstation*) (www.rollei.de), V-STARS/S or RolleiMetric CDW PLUS 750, which are used in close range photogrammetry applications. Those systems are based on more open, hybrid photogrammetric data processing tools with user friendly interfaces. However, they are very costly, and therefore the alternative less expensive photogrammetric approaches are applied with the use of semi-metric digital cameras for acquisition of the images. Non-metric cameras have frequently been employed in various projects, concerning different applications, e.g. in architectural and archaeological heritage recording, where usually not so rigid accuracy is required.

For obtaining high precision measurements of surfaces of the 3D small details, an appropriate camera has to be very carefully selected. From the economy point of view, the price of the camera must be reasonable. However, the camera parameters must make possible of taking very large scale photographs (from about 1:25 to 1:50), with the photographic distance ranged from 0.5 m to 1.5 m. The camera should be of a good quality with the stable interior orientation, including that related to the lens distortion. In case of the very large scale photography taken for the objects, the calibration of the camera should be carried out under the similar conditions, since the parameters of interior orientation are significantly changing with the change of the short photographic distance. That requires the use of small size calibration tests which fit to the large scale photographs of small measured objects. The results of the calibration, which are presented by the authors in the following chapters, have been used for precise reconstruction and modelling of over thirty digital surface models for small fragments (3D contact surfaces) of the broken archaeological items.

2. Potentiality of semi-metric cameras

The digital cameras, as the successors of film cameras, day by day are becoming more and more capable. In the consumer market, the new image sensors are being improved, raising the sizes up to 36×24 mm and resolution of over 10 Mpix, with almost microscopic focus mechanisms. The sensors are being improved and becoming less expensive. The suitable camera for very close range photogrammetric measurements should be of a reflex-type with the exchangeable fixed focal lenses, manual and automatic steering and high information capacity, that depends on high resolution and proper parameters (sampling, quantization) of the image analyser with considerable noise reduction. The theoretical accuracy of imagery is estimated as the size of the sample (pixel) in 1 m distance from a camera with the focal length of the lens equal to longer size of the analyser (36 mm). The above characteristics of the cameras do affect their market price. The relation between the images theoretical accuracy and the price of the cameras is shown in Figure 1.

Figure 1 shows that for the reasonable price of US \$2000 it is possible to purchase the semi-metric camera with the object pixel size within 0.35–0.40 mm. However, in case of the use of such a camera for very large scale photography of small objects of variable sizes and depths, not only one basic lens but also some additional lenses are needed. In some extreme exposure conditions, besides automatic function for the compromising setting of the exposure parameters (f -number, exposure time) also a manual one would be beneficial. Various small details (archaeological, industrial) made from different materials, not always can be illuminated, if necessary, by the artificial light because of the light reflection. In such case the compromise is needed; either the longer exposure time or the smaller N -number (it means the larger diameter of lens opening for which the depth of field dD is limited) is required. However, at the same time it is also necessary to satisfy the acquisition of the entire image of the three-dimensional object, being exposed from the short photographic distance D ,

uniformly sharp (within the diameter r of dispersion circle not exceeding 0.02 mm \approx 1.5 pixel). The relation of those parameters for a camera with the focal length c_k is represented by the following equation:

$$dD = \frac{2 \cdot D \cdot c_k^2 \cdot (D - c_k) \cdot N \cdot r}{c_k^4 \cdot N^2 \cdot r^2 \cdot (D - c_k)^2} \tag{1}$$

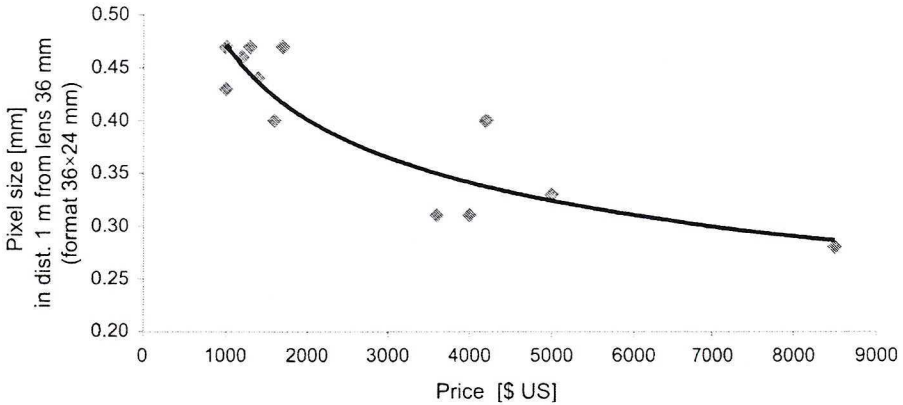


Fig. 1. Relation between the theoretical accuracy of imagery described by the pixel in the object unit and the price for 11 cameras

The analysis of the above relation is particularly important when the 3D objects are exposed from the short photographic distances and all their details are supposed to be uniformly sharp. The depth of field (object) estimated for three lenses with focal lengths of 20 mm, 28 mm, 35 mm, various large photo scales and three different N-numbers are presented in Table 1.

Table 1. Depth dD of field (object) [cm] for different N -number and scales of photo for three lenses and with $r = 0.02$ mm (\approx 1.5 pixel)

| Lens c_k [mm] | $N = 2$ | $N = 5.6$ | $N = 8$ | $N = 2.8$ | $N = 5.6$ | $N = 8$ |
|-----------------|---------------------------------|-----------|---------|---------------------------------|-----------|---------|
| 20 | photo scale 1 : 25 $D = 50$ cm | | | photo scale 1 : 40 $D = 80$ cm | | |
| | 7 | 14 | 20 | 18 | 37 | 55 |
| 28 | photo scale 1 : 25 $D = 70$ cm | | | photo scale 1 : 35 $D = 100$ cm | | |
| | 7 | 14 | 20 | 14 | 28 | 41 |
| 35 | photo scale 1 : 30 $D = 100$ cm | | | photo scale 1 : 35 $D = 150$ cm | | |
| | 9 | 18 | 26 | 20 | 41 | 60 |

Table 1 shows that for the 3D object with the depth up to several centimetres (such objects are assumed to be measured) and the photo scale of 1:25, the N -number should not be smaller than 5.6.

The potentiality of the semi-metric digital cameras together with the particular requirements for the executed research project, concerning the generation of the high accuracy digital surface models (DSM), were major factors when determining the choice of the camera. The Canon EOS 20D camera with three lenses of 20 mm, 28 mm, and 35 mm was purchased by the Institute of Photogrammetry and Cartography of the Warsaw University of Technology, within the research project on numerical modelling of the fragments of the archaeological museum pieces for reconstruction of the original context of the relic (Bujakiewicz et al., 2004–2006).

3. Methods for calibration of very close range cameras

Methods of calibration of non-metric cameras have been developing for many years, even when only the analogue cameras were available (e.g. Karara, 1972; Faig, 1975; Tokarczyk, 1982; Bujakiewicz, 1984). Last few years, those and new methods have also been implemented for calibration of digital non-metric cameras (e.g. Habrouk et al., 1996; McIntosh, 1996; Sawicki, 2001; Tokarczyk and Boroń, 2000; Devernay and Faugeras, 2001; Kager et al., 2002; Kowalczyk, 2003; Podlasiak, 2004; Xie et al., 2004; Cardenal et al., 2004; Grammatikopoulos et al., 2004).

Calibration of a camera used for very large scale photographs is the specific case, since the interior parameters of the camera, including the effect of the image systematic errors, are significantly changing with the change of the photographic distance. This is obviously not the case when the object is exposed from the longer distance and the camera lens is focused for infinity. Therefore, the process of calibration should be carried out for the particular short focusing distances, adequate to those which would be applied to the measurements of an object. The shapes of the 3D small objects require high accuracy photogrammetric measurement. Therefore, the accuracy of determination of parameters of the camera interior orientation has to satisfy very accurate reconstruction of the shapes of the bundles of the image rays. This means, that the focal length c_k and the image principal point (x_0, y_0) as well as the coefficients for the effect of the systematic errors have to be determined in the calibration process under geometric conditions similar to those that would be applied for the object measurement.

The well known mathematical model for the projective rays is described by general collinearity equations, where the parameters of the interior orientation c_k and x_0, y_0 extended by the coefficients for the image systematic errors must be determined for the particular geometric conditions of the camera. The collinearity equations are expressed as:

$$\begin{aligned} (x_{i,j} - x_0) \cdot (1 + \Delta x_{i,j}) &= c_k \cdot F(X_i, Y_i, Z_i, X_j, Y_j, Z_j, \omega_j, \varphi_j, \kappa_j) \\ (y_{i,j} - y_0) \cdot (1 + \Delta y_{i,j}) &= c_k \cdot G(X_i, Y_i, Z_i, X_j, Y_j, Z_j, \omega_j, \varphi_j, \kappa_j) \end{aligned} \quad (2)$$

where X_i, Y_i, Z_i are the coordinates of point i of the calibration test in the test reference system; $X_j, Y_j, Z_j, \omega_j, \varphi_j, \kappa_j$ are parameters of the exterior orientation of the test photograph j ; $x_{i,j}, y_{i,j}$ are the coordinates of the image point i on the photo j ; $\Delta x_{i,j}, \Delta y_{i,j}$ are the corrections to image coordinates for the image point i of the photo j , described by the function for the image systematic errors.

The most common model for the image systematic errors is of the parametric type:

$$\begin{aligned}\Delta x &= \Delta x_a + \Delta x_r + \Delta x_t \\ \Delta y &= \Delta y_a + \Delta y_r + \Delta y_t\end{aligned}\quad (3)$$

The affine effect on image coordinates x and y is described as

$$\begin{aligned}\Delta x_a &= A \cdot (y - y_0) \\ \Delta y_a &= B \cdot (y - y_0) \\ A &= (1 + ds) \cdot \sin(d\beta) \\ B &= (1 + ds) \cdot \sin(d\beta) - 1\end{aligned}$$

with ds – ratio of the scale factor along y axis to the one along x axis for the image coordinate system; $d\beta$ – deviation of the angle between x and y image axes from 90° ; and x, y – uncorrected image coordinates.

Radial distortion effect on image coordinates x and y is expressed as

$$\begin{aligned}\Delta x_{r(i,j)} &= x_{i,j} \cdot (k_1 \cdot r_{i,j}^2 + k_2 \cdot r_{i,j}^4 + k_3 \cdot r_{i,j}^6 + \dots + k_n \cdot r_{i,j}^{2n}) \\ \Delta y_{r(i,j)} &= y_{i,j} \cdot (k_1 \cdot r_{i,j}^2 + k_2 \cdot r_{i,j}^4 + k_3 \cdot r_{i,j}^6 + \dots + k_n \cdot r_{i,j}^{2n})\end{aligned}$$

where $r_{i,j}$ is a radial distance of image point, and k_1, k_2, \dots, k_n are coefficients for the radial distortion.

Tangential distortion effect on image coordinates x and y is described as

$$\begin{aligned}\Delta x_{t(i,j)} &= [p_1 \cdot (r_{i,j}^2 + 2x_{i,j}^2) + p_2 \cdot 2x_{i,j}y_{i,j}] \cdot [1 + p_3r_{i,j}^2 + \dots] \\ \Delta y_{t(i,j)} &= [p_1 \cdot 2x_{i,j}y_{i,j} + p_2 \cdot (r_{i,j}^2 + 2y_{i,j}^2)] \cdot [1 + p_3r_{i,j}^2 + \dots]\end{aligned}$$

where p_1, p_2, \dots, p_n are coefficients for the tangential distortion.

The model described generally above, has been used in many various forms (models of Brown, Torlegard, Bpouer/Mueller, USGS, ISPRS and others) in the photogrammetric practice (e.g. Kager et al., 2002; Gomez Lahoz et al., 2004; Parmehr and Azizi, 2004; Bujakiewicz et al., 2004).

The calibration process requires the use of the proper size calibration tests which fit to the large scale photographs. The type and parameters of the calibration test are the main factors when selecting the calibration procedure. For the purpose of this research, two approaches have been selected, which apply either 3D or 2D calibration tests.

In case of 3D calibration test with the discrete points, their number and distribution should ensure the accurate determination of the calibration parameters. The shape and size of the points (signals) should fit to the scale of photos and be suitable for automatic

measurement of their images. The three-dimensional calibration test, which has been proposed for the purpose of the discussed research project is shown in Figure 2. The test of the size of 500×500 mm is accommodated to perform calibration of the camera with three lenses (20 mm, 28 mm, 35 mm) and for taking photographs at scales from 1:20 to 1:50 (photographic distance from 500 mm to 1500 mm, dependently on scale and type of lens). In the central area of the test, 12 points are distributed within 50 mm depth of field (difference in Z axes of the coordinate system of the calibration test). Within the entire size of the test there are 52 points within 140 mm depth of field.

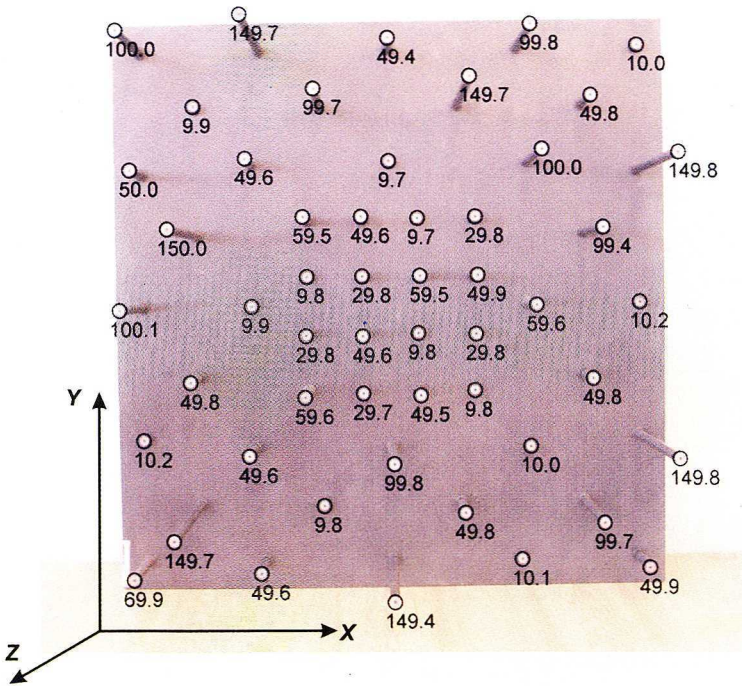


Fig. 2. Three dimensional calibration test for very large close range photographs

The shape and size of the signals are accommodated to semi-automatic and automatic measurement. The test was precisely manufactured and the test reference coordinates of all points were measured with the accuracy of 0.1 mm. The test was exposed on six photos. The parameters of the interior orientation were determined with the calibration computer program, named 'Calib', which is based on the multi images approach. The image coordinates of the 3D calibration test (Fig. 2) were measured in the separate process for all photographs taken.

The second calibration approach (conducted the comparison) was based on the 2D test. This method presented in (Devernay and Faugeras, 2001; Xie et al., 2004; Habib et al., 2004; Podlasiak, 2004) employs the two-dimensional calibration test of the chessboard pattern, with two families of mutually orthogonal parallel lines. The

chessboard test has known geometry and easily detectable feature points, for which the sides of the square areas are known. Such type of the 2D test was exposed in this research project on sixteen photographs, taken from different directions (Fig. 3).

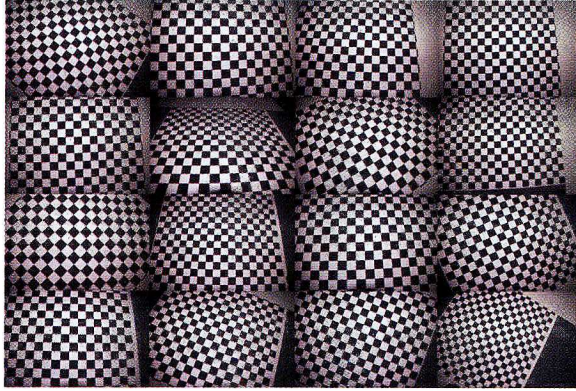


Fig. 3. Sixteen photographs of 2D chessboard calibration test

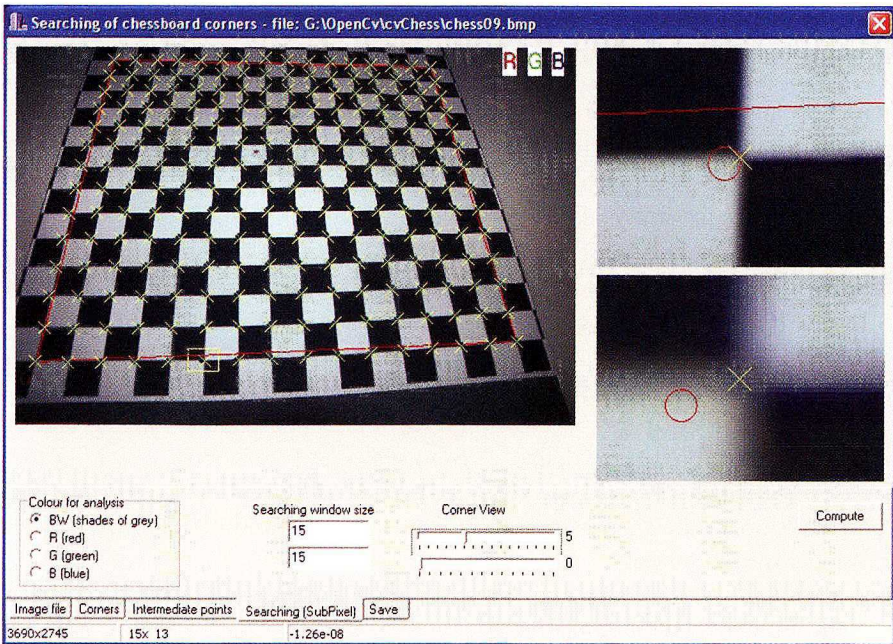


Fig. 4. The program based on the Open Source Computer Vision Library – ‘OpenCv’

The calibration program, developed by Podlasiak (see Fig. 4), has utilized the Open Source Computer Vision Library – ‘OpenCv’, available via internet (www.vision.caltech.edu). The ‘OpenCv’ has built-in support for the chessboard as

a calibration test and it contains the tools for the simultaneous semi-automatic measurement of the images and their processing. The process contains two steps, the initialisation and the adjustment. In the first step, after introducing the number of the chessboard squares and the size of the test area, the automatic measurement of all square corners is carried out with the accuracy of 0.1 pixel.

In the second step, the simultaneous adjustment of observations from all images allows to determine the unknown parameters of the interior orientation.

Both packages are based on the multi-bundles adjustment solution and allow to determine all camera interior orientation parameters, including the coefficients for the image systematic errors.

4. Calibration results and analysis

The Canon EOS 20D camera with three lenses of 20 mm, 28 mm, and 35 mm, was calibrated by two calibration methods 'Calib' and 'OpenCv'. Such choice of methods, has allowed the authors to compare two different approaches, which are based on photographs of the 3D and 2D calibration tests, and to determine independently the same interior orientation parameters. For each of three lenses, the photographs were taken in at least two very large image scales (different short photographic distances). The scales varied from 1:25 to 1:50, according to the type of the lens. This allowed to analyse how the parameters of the interior orientation are changing in the function of the image scale for each of three lenses. The results for the focal length c_k and the coordinates x_0 , y_0 of the image principal point determined by two calibration approaches, are presented in Table 2.

As it is shown in Table 2 and in Figure 5, the differences in the focal length c_k , determined by the two methods 'Calib' and 'OpenCv', are insignificant. They are comprised within the range from 0.007% to 0.65% of the focal length. It is also clearly shown in Figure 5, that for the very large photo scales (indicated on the horizontal axis), for each of three lenses, the focal length c_k (on the vertical axis in pixels), is decreasing with the decreasing of the photo scale (indicated on the horizontal axis), i.e. with the increasing of the photographic distance. The changes in the focal length for different photographic short distances (photo scales 1:25–1:50) are within the range of 30–60 pixels. Such changes in the focal length are significant and must be taken into consideration in the reconstruction of interior orientation during the stage of the object precise measurement.

The results of two calibration methods: 'OpenCv' and 'Calib', in terms of the effect of the image systematic errors, for three lenses (20 mm, 28 mm, and 35 mm), are presented in Figures 6 and 7. For the lens with the focal length of 20 mm, the results are shown for two different photo scales: 1:25 and 1:40. For the remaining two lenses, 28 mm and 35 mm, the results are presented for the photo scales 1:25 and 1:35, respectively. In Figure 6, the graphs indicate the spatial distribution of the resultant effect for radial and tangential distortion, determined by two calibration methods (left side – 'OpenCv', right side – 'Calib'). The distribution of the effect of the systematic

Table 2. Calibration results obtained by ‘Calib’ and ‘OpenCV’ methods for the CANON EOS 20D camera with lenses of 20 mm, 28 mm, and 35 mm (pixel size is about 12 μm)

| Lens c_k [mm] | Photo scale; photogr. distance [m] | Calib [pixels] $x_0; y_0$ c_k | OpenCV [pixels] $x_0; y_0$ c_k | Differences $c_{k(\text{OpenCV})} - c_{k(\text{Calib})}$ [pixels]; [% c_k] |
|-----------------------|--|---------------------------------------|--|---|
| 20 | 1:25 0.50 | -6.00; -26.93 3281.23 | -4.83; -28.42 3275.75 | -5.48; 0.160 |
| 20 | 1:40 0.80 | 6.65; -17.85 3248.79 | 6.09; -17.45 3249.44 | 0.65; 0.020 |
| 20 | 1:50 1.0 | -3.92; -27.46 3227.49 | -4.52; -27.19 3227.68 | 0.19; 0.006 |
| 28 | 1:25 0.70 | -22.73; -24.38 4536.97 | -23.09; -20.73 4533.83 | -3.14; 0.070 |
| 28 | 1:35 1.0 | -22.04; -30.23 4491.60 | -17.73; -30.33 4496.35 | 4.75; 0.100 |
| 35 | 1:30 1.0 | 26.15; 2.16 5671.17 | 28.19; -8.13 5670.78 | -0.39; 0.007 |
| 35 | 1:35 1.5 | 38.07; -24.74 5623.97 | 36.83; -22.39 5624.31 | 0.34; 0.006 |

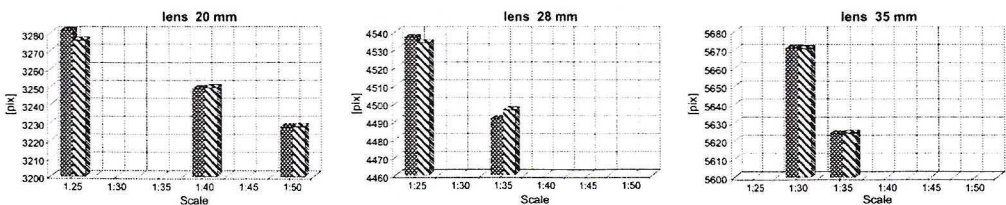


Fig. 5. Comparison of the focal lengths for three lenses (20 mm, 28 mm, and 35 mm), determined by ‘Calib’ and ‘OpenCV’ calibration methods for various very large scale photographs

errors is presented in the form of the contour lines with the contour interval of two pixels ($\sim 20 \mu\text{m}$). On the right-hand side of Figure 7, the spatial distribution of the differences in the resultant effect for radial and tangential distortion, determined by two analysed methods is presented in the form of contour lines with a contour interval of half of the pixel. On the left-hand side of Figure 7, the graphs indicate the effect of only radial distortion Δr , determined by two methods (thick black line for ‘Calib’, thin grey line for ‘OpenCV’ and thick grey line for the difference).

From the results shown in Figures 6 and 7, the following observations can be drawn:

- Both calibration methods ‘OpenCv’ and ‘Calib’ provide similar results for the resultant radial and tangential lens distortion for the particular lens and photo scale (Fig. 6 and Fig. 7 – right side). The spatial distribution of the effect of the

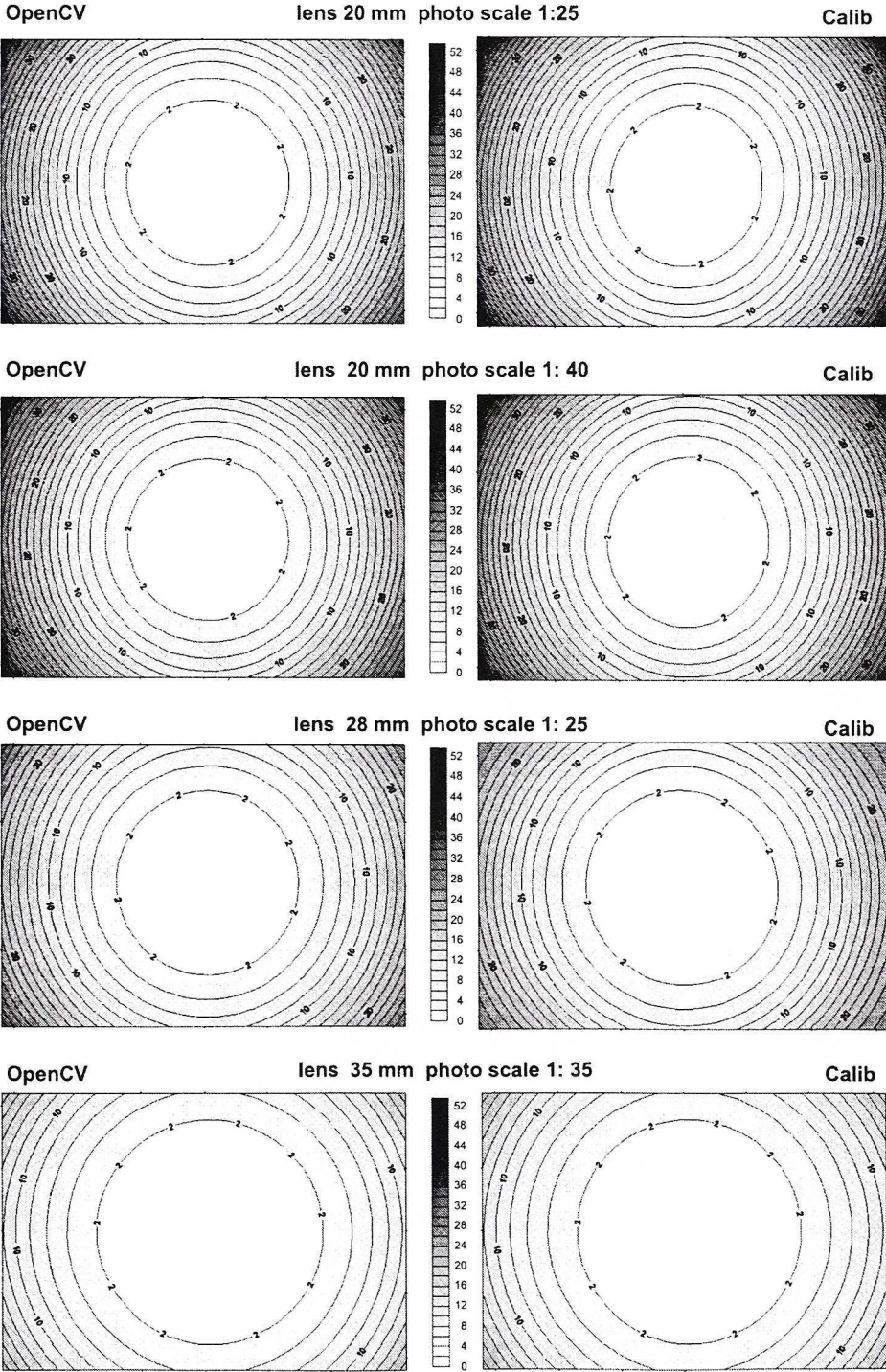
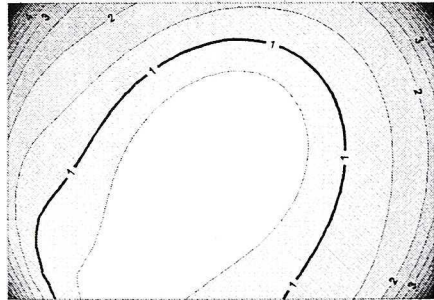
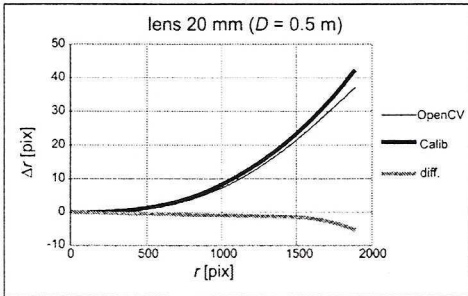


Fig. 6. The results of the effect for radial and tangential distortion determined by two methods [pixels]

effect of radial distortion

lens 20 mm, photo scale 1:25

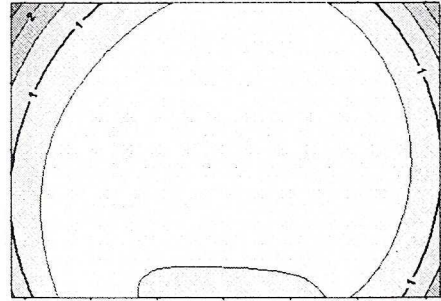
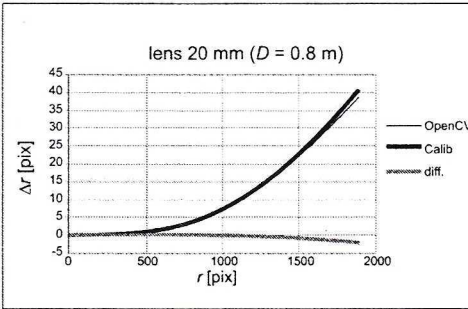
differences OpenCv-Calib in rad. & tang.



effect of radial distortion

lens 20 mm, photo scale 1:40

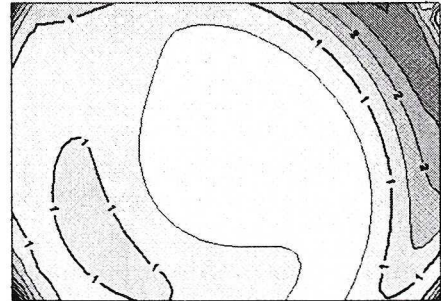
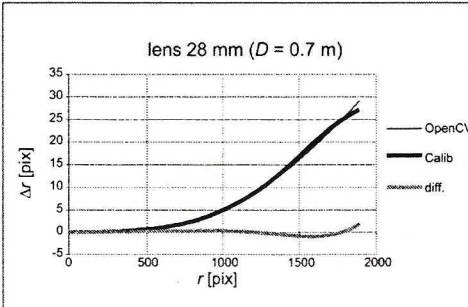
differences OpenCv-Calib in rad. & tang.



effect of radial distortion

lens 28 mm, photo scale 1:25

differences OpenCv-Calib in rad. & tang.



effect of radial distortion

lens 35 mm, photo scale 1:35

differences OpenCv-Calib in rad. & tang.

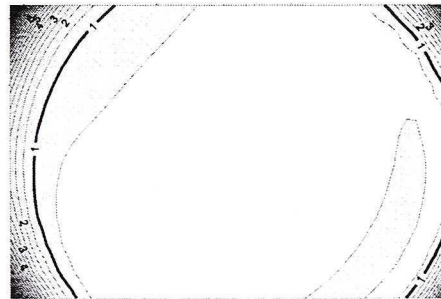
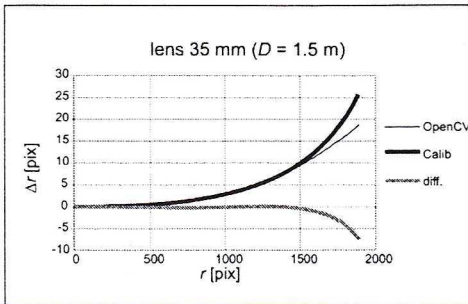


Fig. 7. The results of the effect for radial distortion determined by 'Calib' and 'OpenCv' calibration methods (left side), and the differences in radial and tangential distortion by two methods (right side) [pixels]

resultant radial and tangential distortion (Fig. 6) shows that the radial distortion is predominant. This is consistent with the most of the results obtained in the other projects concerning the calibration of such type of the cameras. The spatial distribution of the effect of distortion for three lenses (20 mm, 28 mm, 35 mm), is slightly different, but all are of symmetrical shapes. There is also slightly different spatial distribution of the differences in the effect of distortion, determined by the two methods (shown as the contour lines), but in the image boundary they do not exceed 1–4 pixels (Figure 7 – right side).

- The effect of the radial distortion determined by two methods (graphs on the left side of Figure 7) is very similar for the respective parameters of the photographs (the same lens and scale of the photo). Among three lenses (20 mm, 28 mm, 35 mm), the lens of 20 mm is characterized by the largest effect of the radial distortion, which does not significantly change with the change of a photo scale. For the radial distance of 1800 pixels (the image boundary), the effect of the lens radial distortion has reached 40 pixels for both photo scales: 1:25 and 1:40. Similar magnitude of pixels can be observed from the spatial distribution of the resultant radial and tangential distortion graph (Fig. 6). For radial distance of 1000 pixels this effect is about 7–8 pixels. For the lenses of 28 mm and 35 mm, the radial distortions at a radial distance of 1800 pixels are within the range of 25–28 pixels, that is much lower than for the 20 mm lens. For the distance of 1000 pixels they equal to 5 and 2 pixels, respectively.

5. Conclusions

The results of camera calibration obtained in the experiment, have proved the possibility of using two alternative approaches, based on the multi images of either the 3D or 2D test. Both approaches have provided the very similar and accurate interior orientation parameters, including those which describe the image systematic errors.

The comprehensive research has provided the calibration parameters for the Canon EOS 20D camera with three different lenses (20 mm, 28 mm, and 35 mm). The interior orientation parameters of the camera with the above three lenses were determined for different short photographic distances within the range of 0.7–1.5 m (the image scales 1:25-1:50).

Various sets of the parameters determined in the calibration process (for three different lenses and various photographic distances) were subsequently used for reconstruction of the bundles of rays for the photographs taken (with the lens and geometry adequate to the calibration) for small broken fragments of the archaeological items (statuettes, stone plates, etc.). The accurate interior orientation of the camera available from the calibration as well as the special reference control points structure, have allowed to reconstruct over thirty 3D models of archaeological fragments with the average accuracy of 0.2 mm for each X , Y , Z coordinate.

In conclusion it should be pointed that the use of the semi-metric cameras instead of the very expensive metric digital cameras for the photogrammetric surface modelling

of small features, where the accuracy requirements are very high, is possible and reasonable but the camera and the lenses as well as the camera calibration procedures must be chosen with a special care.

Acknowledgements

The research was supported by the Polish State Committee for Scientific Research as the part of the project KBN T12 E 033 26, on “Numerical modelling of the fragments of the archaeological pieces for the reconstruction of the original context of the relic”. The authors express their sincere gratitude to Prof. J. Jachimski and to anonymous reviewer whose valuable comments led to improve the manuscript of this paper.

References

- Bujakiewicz A., (1984): *Usefulness of Long Focus non Metric Cameras in Precise Measurements*, International Archives of ISPRS, Vol. XXV, B5, pp. 136-140.
- Bujakiewicz A., Kowalczyk M., Podlasiak P., Zawieska D., (2004): *Modelling and Visualization of Three Dimensional Objects Using Close Range Imagery*, The International Archives for Photogrammetry, Remote Sensing and Spatial Information Sciences, Vol. XXXV, B5, pp. 442-446.
- Bujakiewicz A., Kowalczyk M., Podlasiak P., Zawieska D., Rzepka S., (2004–2006): The research project T12 E 033 26, on “*Numerical modelling of the fragments of the archaeological pieces for the reconstruction of the original context of the relic*”, supported by the Polish State Committee for Scientific Research, Reports for 2004 and 2005, Institute of Photogrammetry and Cartography, Warsaw University of Technology.
- Cardenal J., Mata E., Castro P., Delgado J., Hernandez N.A., Peres J.L., Ramos M., Torres M., (2004): *Evaluation of a Digital Non Metric Camera (Canon D30) for the Photogrammetric Recording of Historical Buildings*, Archives of Photogrammetry and Remote Sensing, Vol. XXXV, B5, pp. 445-460.
- Devernay F., Faugeras O., (2001): *Straight lines have to be straight. Automatic calibration and removal of distortion from scenes of structured environments*, Machine Vision and Applications 13, pp. 14-24.
- Faig W., (1975): *Calibration of Close Range Photogrammetric Systems – Mathematical Formulation*, Archives of XIII ISPRS Congress, Helsinki, pp. 1479-1486.
- Gomez Lahoz J., Cuadrado Mendez O., Martinez Rubio J., (2004): *Lens Distortion Simulation, an Application for Understanding Geometric Distortion*, Archives of Photogrammetry and Remote Sensing, Vol. XXXV, B5, Supplement.
- Grammatikopoulos L., Karras G., Petsa E., (2004): *Camera calibration combining images with two vanishing points*, Archives of Photogrammetry and Remote Sensing, Vol. XXXV, B5, pp. 99-104.
- Habrouk H.E., Li X.P., Faig W., (1996): *Determination of Geometric Characteristics of a Digital Camera by Self-Calibration*, International Archives of Photogrammetry and Remote Sensing, Vol. XXXI, Part B1, Vienna, pp. 60-64.
- Habib A.P., Ghanma R.J., Kim E.M., (2004): *3D Modelling of Historical Sites using Low Cost Digital Cameras*, Archives of Photogrammetry and Remote Sensing, Vol. XXXV, B5, pp. 570-575.
- Kager H., Rottensteiner F., Kerschner M., Stadler T., (2002): *ORPHEUS 3.2.1 User Manual*, Institute of Photogrammetry and Remote Sensing, Vienna University of Technology.
- Karara H.M., (1972): *Simple Cameras for Close Range Applications*, Photogrammetric Engineering, Vol. 38, No 5.

- Kowalczyk M., (2003): *Investigation on Possibilities of Automation in Photogrammetric Measurement with use of Digital Camera* (in Polish), PhD theses, Institute of Photogrammetry and Cartography, Warsaw University of Technology (133 pp).
- McIntosh K., (1996): *A Calibration Procedure for CCD Array Cameras*, International Archives of Photogrammetry and Remote Sensing, Vol. XXXI, Part B1, Vienna, pp. 138-143.
- Parmehr E.G., Azizi A., (2004): *A comparative evaluation of the potential of close range photogrammetric technique for the 3D measurement of the body of a Nissan petrol car*, Archives of Photogrammetry and Remote Sensing, Vol. XXXV, B5, pp. 110-113.
- Podlasiak P., (2004): *Determination of Camera Distortion on the Basis of Images of the Natural Objects* (in Polish), Archiwum Fotogrametrii, Kartografii i Teledetekcji, Vol. 14, pp. 459-466.
- Sawicki P., (2001): *Solution of Terratriangulation with Self-calibration of Digital Camera Kodak DC4800* (in Polish), Archiwum Fotogrametrii, Kartografii i Teledetekcji, Vol. 11, pp. 3/25-3/32.
- Tokarczyk R., (1982): *Investigation on the Use of Non-metric Cameras in Precise Measurements for Engineering* (in Polish), PhD theses, Faculty of Mining Surveying and Environmental Engineering, AGH – University of Science and Technology in Cracow (87 pp).
- Tokarczyk R., Boroń A., (2000): *Investigation on the Use of Non-metric Cameras for Photogrammetric Applications* (in Polish), Archiwum Fotogrametrii, Kartografii i Teledetekcji, Vol. 10, pp. 63/1-63/10.
- Xie W., Zhang Z., Zhang J., (2004): *Multi based camera calibration without control point*, Archives of Photogrammetry and Remote Sensing, Vol. XXXV, B5, pp. 36-41.
[www.rollei.de]

Kalibracja kamer cyfrowych bardzo bliskiego zasięgu

Aleksandra Bujakiewicz, Michał Kowalczyk, Piotr Podlasiak, Dorota Zawieska

Instytut Fotogrametrii i Kartografii
Politechnika Warszawska

Plac Politechniki 1, 00-661 Warszawa

e-mail: abujak7@wp.pl, mmkowalczyk@wp.pl, ppodlasiak@wp.pl, dorotaz8@wp.pl

Streszczenie

Artykuł dotyczy procesu kalibracji semi-metrycznych kamer cyfrowych. Stosując takie kamery do pomiaru małych obiektów, zdjęcia muszą być wykonane w bardzo dużej skali, w zakresie od około 1:20 do 1:50. W celu zapewnienia dokładności pomiaru fotogrametrycznego na poziomie poniżej pół milimetra, należy stosować specjalne procedury i testy kalibracyjne dla określenia parametrów orientacji wewnętrznej, łącznie ze współczynnikami opisującymi błędy systematyczne zdjęć. W niniejszym artykule, przedstawiono porównanie dwóch metod, bazujących na obrazach dwuwymiarowych i trójwymiarowych testów kalibracyjnych. Wykonany eksperyment jest częścią projektu badawczego, finansowanego przez KBN, który dotyczy numerycznego modelowania fragmentów rzeźb w celu rekonstrukcji oryginalnego kontekstu zabytku.